



Adsorption of cadmium onto modified nanosized magnetite: kinetic modeling, isotherm studies, and process optimization

Ali Akbar Babaei^{a,b}, Mehdi Bahrami^{c,*}, Ahmad Farrokhian Firouzi^d, Amirhosein Ramazanpour Esfahani^d, Leila Alidokht^e

^aEnvironmental Technologies Research Center, Ahvaz Jundishapur University of Medical Sciences, Ahvaz, Iran, email: babaei-a@ajums.ac.ir (A.A. Babaei)

^bDepartment of Environmental Health Engineering, School of Public Health, Ahvaz Jundishapur University of Medical Sciences, Ahvaz, Iran

^cFaculty of Agriculture, Department of Water Engineering, Fasa University, Fasa, Iran, Tel. +98 715 3340519; Fax: +98 715 3342520; email: bahrami@fasau.ac.ir (M. Bahrami)

^dFaculty of Agriculture, Department of Soil Science, Shahid Chamran University, Ahvaz, Iran,

emails: a.farrokhian@scu.ac.ir (A. Farrokhian Firouzi), ramazanpour67@gmail.com (A. Ramazanpour Esfahani)

^eFaculty of Agriculture, Department of Soil Science, University of Tabriz, Tabriz, Iran, email: alidokht_68@yahoo.com (L. Alidokht)

Received 28 April 2014; Accepted 16 September 2014

ABSTRACT

In this study, adsorptive removal of cadmium(II) from aqueous solutions using sodium dodecyl sulfate-modified magnetite nanoparticles was modeled. To this aim, central composite design as one of the most favorable designs in response surface methodology (RSM) was employed to optimize the removal of Cd(II) from solution under different variables such as adsorbent dosage (0.1–0.55 g), initial ion concentration (6–90 mg/L), and reaction time (5–30 min). Furthermore, the experimental data of Cd(II) adsorption were tested with various kinetic and isotherm models at various initial ion concentrations of 10–50 mg/L and adsorbent dosages of 0.1–0.25 g. The adsorption process followed the intra-particle diffusion model ($R^2 > 0.94$) very well. The equilibrium adsorption data were analyzed using various isotherm models. The results showed that Freundlich isotherm, with a relatively high coefficient of determination ($R^2 > 0.96$), fits well with the experimental results of Cd(II) adsorption. Ultimately, the optimum Cd(II) ions removal of 91.07% was obtained at the reaction time of 30 min, the adsorbent dosage of 0.35 g, and the initial ion concentration of 30 mg/L.

Keywords: Cadmium; Central composite design; Isotherm; Kinetic; Magnetite; Response surface methodology

1. Introduction

Heavy metal pollution of wastewater is always considered as the most common environmental threat due to the fact that venomous metal ions are poten-

tially able to reach the top of the food chain and thus become a risk agent for human health [1–4]. In this regard, cadmium(II) is a toxic ion with significant environmental and occupational concerns [5,6]. It has been released to soil and water sources through the combustion of fossil fuels, production of metals, application of

*Corresponding author.

phosphate fertilizers, and electroplating and manufacturing of batteries, pigments, and screens [5,7,8].

Nowadays, numerous methods have been proposed for the efficient removal of heavy metal ions from aqueous solutions, including as chemical precipitation, ion exchange, adsorption, membrane filtration and electrochemical technologies [9,10]. From among these techniques, adsorption is not only an attractive and cost-effective technology but it is also flexible in design and operation, and in many cases, it generates high-quality treated effluents [11–24]. A large number of adsorbents, such as clays [7], dried plant parts [25], agricultural waste biomass [26,27], metal oxides [28], sewage sludge [29], saw dust [30], charred biomaterials [31], microorganisms, fly ash [32], and zeolites [33], have so far been employed to remove cadmium from either water or soil environments. In comparison with conventional adsorbents, magnetic nanoparticles can be manipulated or recovered swiftly using an external magnetic field. Moreover, they enjoy satisfying efficiency owing to a highly efficient specific surface area [34].

Inorganic nanoparticles, in particular, are susceptible to aggregate into micron or even larger particles because of direct particle–particle interactions such as van der Waals forces and magnetic attraction. Aggregation, it is believed, possibly reduces the specific surface area and the interfacial free energy, thereby dropping reactivity of and spoiling the unequaled features of nanoparticles [35]. In order to either prevent or decrease the agglomeration of nanoparticles, various stabilizers have been found to be effective for stabilizing nanoparticles, including clay minerals [36], carboxylic acids [37], and polymers [38,39].

Logically, the performance of nanoparticles in adsorption of Cd(II) is dependent upon several experimental variables. To examine each independent factor, the other variables should certainly be kept constant, which may lead to increasing the number of experiments. Therefore, it seems to be a critical approach to minimize the number of batch experiments and optimize them in order to cut down on the costs of research and time. Response surface methodology (RSM) comprises a bunch of mathematical and statistical methods to examine and model any problem in which dependent parameters are highly affected by a group of independent factors [40]. The most important advantage that distinguishes RSM from other traditional approaches is a decrease in the number of experiments so that it provides sufficient information for statistically valid results and evaluates the relative significance of parameters and their interactions [41]. Two most common designs extensively used in RSM are the central composite design (CCD) and the Box–Behnken design. The CCD is immensely

appropriate for sequential experimentation and allows a reasonable amount of information for testing the lack of fit while not involving an unusually large number of design points [42].

The main objectives of the present study were as follows: (1) the synthesis and characterization of sodium dodecyl sulfate-modified magnetite nanoparticles (labeled as SDS-MNP) (2) the optimization and modeling of Cd(II) adsorption onto SDS-MNP using CCD with RSM, and (3) the isotherm and kinetic investigations of cadmium removal from the aqueous solutions by SDS-MNP. In this research, CCD was used to develop a mathematical correlation between cadmium removal efficiency and three other chosen independent variables including the adsorbent dosage (g), the initial ion concentration (mg/L), and the reaction time (min).

2. Materials and methods

2.1. Chemicals

The ferric chloride hexahydrate ($\text{FeCl}_3 \cdot 6\text{H}_2\text{O}$) and sodium dodecyl sulfate (SDS) ($\text{NaC}_{12}\text{H}_{25}\text{SO}_4$) were purchased from AppliChem Co. However, cadmium nitrate ($\text{Cd}(\text{NO}_3)_2$), acetone, sodium hydroxide, and hydrochloric acid were prepared from Merck Co. All the chemicals applied in this study were of analytical grade. In addition, deionized water was used to prepare any of the aqueous solutions. For the preparation of cadmium solution, desired amounts of cadmium nitrate were poured in deionized water and consequently diluted in appropriate concentrations.

2.2. Synthesis and characterization of SDS-MNP

The modified magnetic nanoparticles were synthesized in line with the method described by Si et al. [43]. Briefly, 50 mL of ferric chloride solution was added dropwise to 50 mL of SDS solution (0.625 w/v). The obtained solution was stirred gently for 30 min to reach the monotonous SDS-Fe solution. Then, the pH of the above-mentioned solution was set at 12 using 0.5 M of sodium hydroxide solution (0.5 M NaOH) and shaken with a constant rate for 1 h. When the reaction ended, the resulted nanoparticles were extracted from the suspension using a 1.6 Tesla magnet and dried in oven at 50°C. Afterward, the dried particles were kept in 0.1 M NaOH for 15 min, then washed sequentially with deionized water, and finally kept at 50°C for over 12 h.

The size and structure of synthesized magnetite nanoparticles were determined using scanning electron microscope (SEM, Philips, The Netherlands).

Additionally, crystalline features of nanoparticles were measured via X-ray diffraction (XRD, Hitachi PW 4160, Japan) between 2θ of 20–70°. The XRD diagram was obtained using Cu $k\alpha$ radiation source (40 kV, 35 mA) at $\lambda = 0.154$ nm.

2.3. The experimental procedure

To optimize the treatment of simulated Cd-contaminated solution, a series of batch experiments in several bottles were carried out under different experimental variables including the reaction time (6–30 min), the adsorbent mass (0.1–0.55 g), and the initial Cd(II) concentration (6–90 mg/L). All the experiments were conducted in room temperature ($25 \pm 1^\circ\text{C}$). The bottles containing the mixture of Cd(II) solution with magnetite nanoparticles were shaken at 120 rpm using a rotary orbital shaker. The optimum pH value of the batch

experiments was 6.0. This was obtained from the pre-experiments and was consequently used in all the optimization, kinetic, and isotherm experiments of Cd(II) adsorption. In the final stage of batch experiments, the SDS-MNP were separated from the solutions using a permanent magnet and the initial and final metal concentrations were determined by a flame atomic absorption spectrometer (Analytic Jena, Vario 6, Germany).

The adsorption efficiency (%R) and the adsorption capacity (q) (mg/g) of cadmium using SDS-MNP were calculated using Eq. (1) and (2), respectively [44]:

$$\%R = \frac{C_0 - C_e}{C_0} \times 100 \quad (1)$$

$$q = \frac{C_0 - C_e}{m} \times V \quad (2)$$

Table 1
Mathematical equations of the used kinetic and isotherm adsorption models

Model	Equation	Parameter and dimension
<i>Kinetic models</i>		
Pseudo first-order (Lagergerm)	$q_t = q_e(1 - \exp(-k_f t))$	K_f (1/min)
Pseudo second-order (Ho)	$q_t = \frac{k_s q_e^2 t}{1 + q_e k_s t}$	q_e, q_t (mg/g) k_s (mg/g min)
Intra-particle diffusion	$q_t = k_{id} t^{1/2} + C$	t time (min) k_{id} (mg/g min ^{0.5}) C (-)
Fractional power	$q_t = at^b$	a (mg/g min ^b), b (-)
<i>Isotherm models</i>		
Langmuir	$q_e = \frac{b q_{max} C}{1 + b C}$	q_{max} (mg/g) b (L/mg)
Freundlich	$q_e = K_F C_e^{1/n}$	K_F (mg/g) (mg/L) ⁻ⁿ n model exponent (-)
Langmuir–Freundlich (L–F)	$q_e = \frac{q_{max} (b C_e)^n}{1 + (b C_e)^n}$	n (-) ($0 < n < 1$)
Redlich–Peterson (R–P)	$q_e = \frac{K_R C_e}{1 + a_R C_e^\beta}$	K_{RP} (L/g) a_{RP} (L/mg) β (-) ($0 < \beta < 1$)

Table 2
The experimental range of input parameters in CCD

Variables (factors)	Ranges and actual values of coded levels				
	-1.682	-1	0	+1	+1.682
Adsorbent dosage (g) (X_1)	0.1	0.2	0.33	0.46	0.55
Initial ion concentration (mg/L) (X_2)	6	23	48	73	90
Reaction time (min) (X_3)	5	10	17	25	30

where C_e and C_0 are the concentration in equilibrium and the initial concentration of Cd(II) in solution (mg/L), respectively. V is the volume of solution (L) and m is the mass of the adsorbent (g).

2.4. Mathematical modeling study

2.4.1. Adsorption kinetic models

In this study, four common kinetic models including pseudo-first-order of Lagergren [45], pseudo-second-order of Ho [46], fractional power (F-P) [47], and intra-particle diffusion (I-D) [48] were applied to fit the experimental data of Cd(II) removal using modified magnetite nanoparticles. All the employed mathematical kinetic models are summarized in Table 1, where q_e and q_t (mg/g) are the adsorption capacities at equilibrium and at time t , respectively. The parameters k_f (1/min) and k_s (g/mg min) are the rate coefficients for pseudo-first-order and pseudo-second-order kinetic models, respectively. k_{id} (mg/g min^{0.5}) is the constant rate of I-D, and C is the constant which depicts the boundary layer effects. Finally, a (mg/g min^b) and b are the F-P kinetic model constants.

2.4.2. Adsorption isotherm models

In order to express the isotherm study of Cd(II) removal from aqueous solutions using SDS-MNP, four widely used isotherm models including Freundlich, Langmuir, Redlich–Peterson (R–P), and Langmuir–Freundlich (L–F) were applied. The Freundlich isotherm model is an appropriate model for the non-ideal adsorption of adsorbates onto the heterogeneous reactive sites of adsorbents as well as the multilayer adsorption [49]. The hypothesis of Langmuir isotherm is based on the adsorption of adsorbate onto the reactive sites of the adsorbent, with the adsorption being impeded by filling of the surface layer of the adsorbent with adsorbates [9]. Furthermore, the model was found necessary by means of a typical constant known as R_L dimensionless separation factor, which can be obtained using Eq. (3) [50]:

$$R_L = \frac{1}{1 + bC_0} \quad (3)$$

where C_0 is the initial adsorbate concentration in bulk solution (mg/L) and b is the isotherm constant. Based on a general protocol, $R_L > 1$ implies an unfavorable adsorption. However, R_L between 0 and 1 shows an extremely favorable condition in the adsorption process. Finally, $R_L = 0$ shows an irreversible adsorption status.

Table 1 shows the employed mathematical isotherm models, where q is the adsorbed amount and C_e is the equilibrium concentration of Cd(II). In the Langmuir model, q_m is the maximum solute adsorbed at the equilibrium state for the completion of a layer (mg/g) and b is a constant that depends on the energy of adsorption which shows the enthalpy of adsorption. It is also an index to describe the binding energy of surface adsorption. In the Freundlich model, K_F and n are the coefficients attributed to the adsorption capacity and the adsorption intensity of adsorbent, respectively. In the L–F model, b (L/mg) and n are the coefficients attributed to the L–F equilibrium constant and the exponent of the L–F equation, respectively [51]. K_R , a_R , and β in the R–P isotherm are the model constants. K_R is the solute adsorptivity (L/g), a_R is relevant to the adsorption energy (L/mg), and β is the heterogeneity constant ($0 < \beta < 1$) [52].

2.5. Central composite design

To optimize the adsorptive removal of Cd(II) from solutions using SDS-MNP, CCD was applied under different experimental factors including the adsorbent

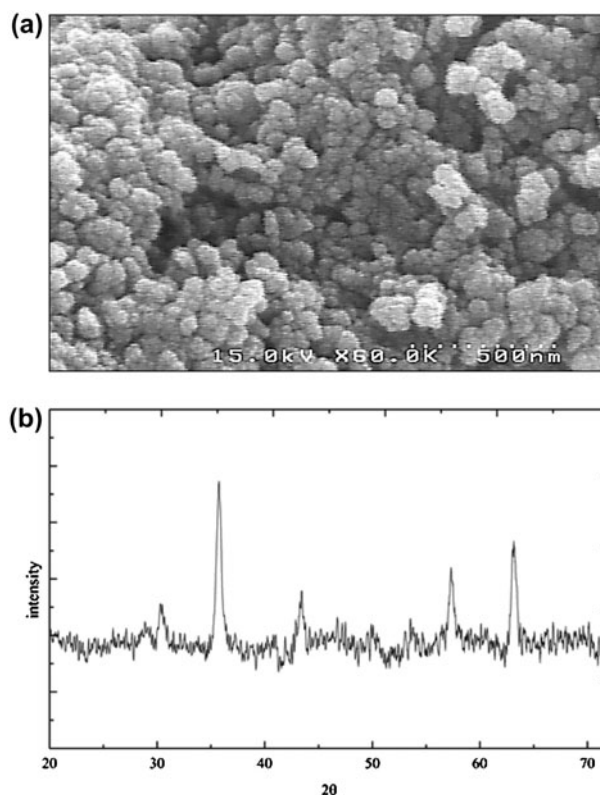


Fig. 1. (a) SEM image and (b) XRD diagram of SDS-MNP.

dosage (g), the initial ion concentration (mg/L), and the reaction time (min). The experimental ranges of the applied variables are reported in Table 2. A total of 20 experiments were conducted: eight at factorial points, six at axial points, and six at central points.

In order to do the statistical analyses, the parameters X_i (the actual amounts of an independent factor) were coded as x_i (dimensionless values of the dependent factor) via Eq. (4):

$$x_i = \frac{X_i - X_0}{\delta X} \quad (4)$$

where X_0 is the quantity of X_i at the central point and δX is the step change.

The response variables were fitted using the second-order polynomial equation (Eq. (5)) as follows:

$$y = b_0 + \sum b_i x_i + \sum b_{ii} x_i^2 + \sum b_{ij} x_i x_j + \varepsilon \quad (5)$$

where y is the response factor of Cd(II) adsorption efficiency, b_0 is the constant, and b_i is defined as the linear effect of factor x_i ($i = 1, 2,$ and 3). Furthermore, b_{ii} is the squared effect of factors, and b_{ij} is the regression coefficient for the interaction impacts.

The validity of the applied model was examined using the analysis of variance (ANOVA). The statistical significance of model was tested by Fisher's variation ratio (F -test), p -value, and the coefficient of determination (R^2).

The significance of the obtained coefficients was evaluated using the F -test at 95% confidence level. The Pareto graph is depicted using Eq. (6) to obtain the impact of each independent factor and its interaction influence as follows [53]:

Table 3

Experimental and predicted responses of the model for Cd(II) adsorption using SDS-MNP

Run number	Adsorbent dosage (g)	Initial ion concentration (mg/L)	Reaction time (min)	Cadmium adsorption (%)		
				Experimental	Predicted	Residual
1	0.46	29.03	10.07	75.48	79.71	-4.23
2	0.33	12.00	17.50	87.4	79.86	7.54
3	0.46	78.97	10.07	55.81	54.29	1.52
4	0.33	54.00	17.50	71.43	70.7	0.73
5	0.33	54.00	17.50	70.72	70.7	0.02
6	0.10	54.00	17.50	23.6	22.83	0.77
7	0.33	54.00	17.50	69.38	70.7	-1.32
8	0.33	54.00	17.50	70.26	70.7	-0.44
9	0.33	54.00	17.50	70.11	70.7	-0.59
10	0.33	54.00	5.00	51.83	53.02	-1.19
11	0.19	78.97	10.07	30.76	29.3	1.46
12	0.33	54.00	17.50	71.05	70.7	0.35
13	0.19	29.03	24.93	51.78	57.66	-5.88
14	0.33	54.00	30.00	83.02	75.67	7.35
15	0.33	96.00	17.50	41.18	42.56	-1.38
16	0.19	29.03	10.07	40.53	40.82	-0.29
17	0.46	29.03	24.93	91.4	97.22	-5.82
18	0.46	78.97	24.93	60.31	64.38	-4.07
19	0.19	78.97	24.93	38.6	38.73	-0.13
20	0.55	54.00	17.50	82.5	77.11	5.39

Table 4

The ANOVA of the experimental results of CCD

Source of variation	Sum of squares	Degree of freedom	Adjusted mean square	F-value
Regression	6,952.81	9	752.53	33.39
Residual	254.49	11	23.13	
Total	7,207.3	20		

Note: $R^2 = 0.9646$ and $\text{Adj-}R^2 = 0.9357$.

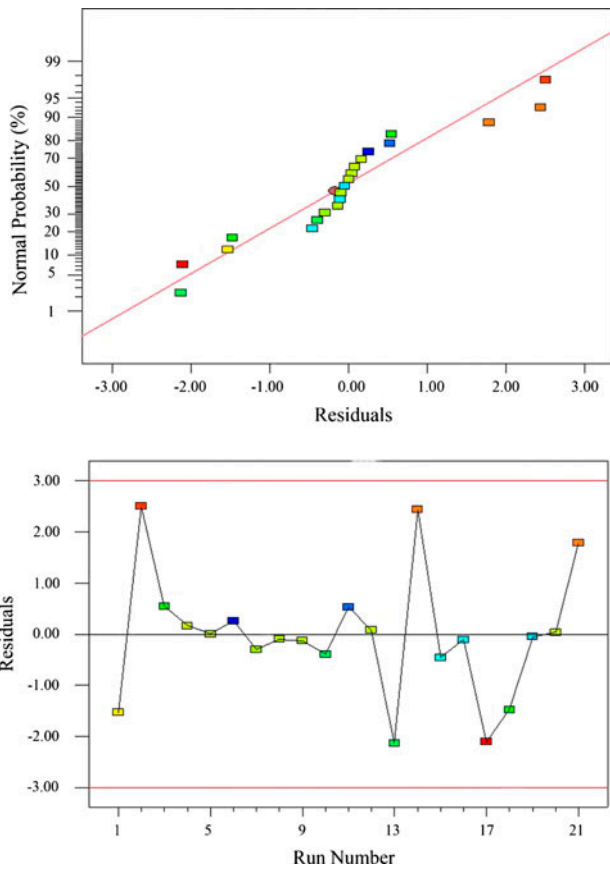


Fig. 2. Residual graphs for Cd(II) adsorption.

Table 5

The obtained regression coefficients corresponding to the model based on experimental variables

Coefficients	Parameter estimate	F-value	p-value
b_0	70.69	33.39	<0.0001
b_1	16.13	153.72	<0.0001
b_2	-11.08	72.58	<0.0001
b_3	6.73	26.76	0.0003
b_{12}	-3.47	4.17	0.0656
b_{13}	0.16	0.01	0.9239
b_{23}	-1.85	1.18	0.299
b_{11}	-7.33	34.85	0.0001
b_{22}	-3.35	7.30	0.0205
b_{33}	-2.24	3.27	0.0976

$$p_i = \left(\frac{b_i^2}{\sum b_i^2} \right) \times 100, \quad i \neq 0 \quad (6)$$

All calculations for obtaining the responses were performed using Design-Expert (Version 8.0.0) software. Furthermore, the interactive impacts of

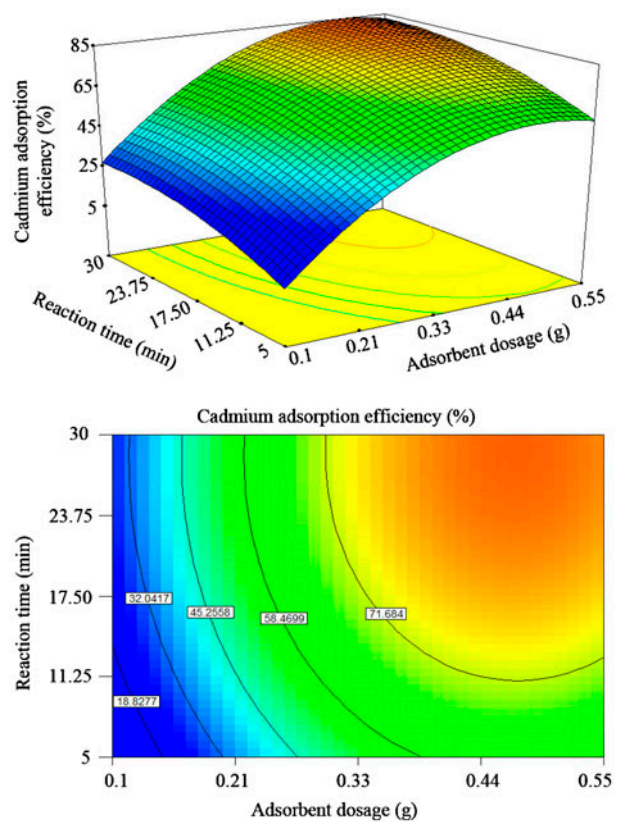


Fig. 3. Response surface and contour plots of interaction effects of reaction time and adsorbent dosage on Cd(II) adsorption.

independent factors on the response were depicted using the two- and three-dimensional plots.

3. Results and discussion

3.1. Characterizations of SDS-MNP

Fig. 1(a) illustrates the SEM image of SDS-MNP. As can be seen from Fig. 1(a), synthesized nanoparticles have a spherical structure in a size range of 40–60 nm. The XRD diagram of nanoparticles is shown in Fig. 1(b). Accordingly, several diffraction peaks in 30.30, 35.67, 43.30, 57.17, 62.90, 71.29, and 73.38° were observed, which are attributed to Fe₃O₄.

3.2. CCD results for Cd(II) adsorption

The mathematical model of Cd(II) adsorption efficiency using SDS-MNP as a function of the adsorbent dosage (g) (X_1), the initial ion concentration (mg/L) (X_2), and the reaction time (min) (X_3) based on the coded values is given as follows:

$$y = 70.69 + 16.13X_1 - 11.08X_2 + 6.73X_3 - 3.47X_{12} + 0.16X_{13} - 1.85X_{23} - 7.33X_1^2 - 3.35X_2^2 + 2.24X_3^2 \quad (7)$$

subjected to $-1.682 < X_i < +1.682$.

The CCD results for optimization of Cd(II) removal comprising experimental and predicted values of Cd(II) adsorption are represented in Table 3. In order to ensure the adequacy of the model, one of the promising approaches is the evaluation of the relationship between the predicted and the experimental data. Regarding this, the high coefficient of determination ($R^2 = 0.96$, $\text{Adj-}R^2 = 0.94$) is a logical proof to approve the reliability of this model.

The ANOVA results are shown in Table 4. It is obvious that at the confidence level of 99%, the calculated F -value (33.39) with high discrepancy is higher than the tabulated one (4.95), confirming the validity of the model and its statistical significance. The p -values of each parameter are less than 0.05, which shows the significance of the experimental variables. Additionally,

the adequacy of the model was evaluated using the residuals. According to Fig. 2, the calculated data were located on a straight line which indicated there was no apparent dispersal. Fig. 2 also demonstrated the random and scattered pattern of residuals against the run number and predicted responses. The coefficients of regressions, together with F -values and p -values, have been illustrated in Table 5. As can be seen, coefficients that have a p -value lower than 0.05, at 95% confidence level, are apparently significant.

Besides, based on the Pareto analysis, among all independent variables, the adsorbent dosage (50.63%), the initial ion concentration (23.91%), and the quadratic effect of initial ion concentration (10.45%) have greater influences on the Cd(II) adsorption efficiency.

3.3. Effect of variables on Cd(II) removal efficiency as surface and contour plots

In optimization studies, three-dimensional surface and contour plots are definitely handy graphical instruments which help researchers to visualize the

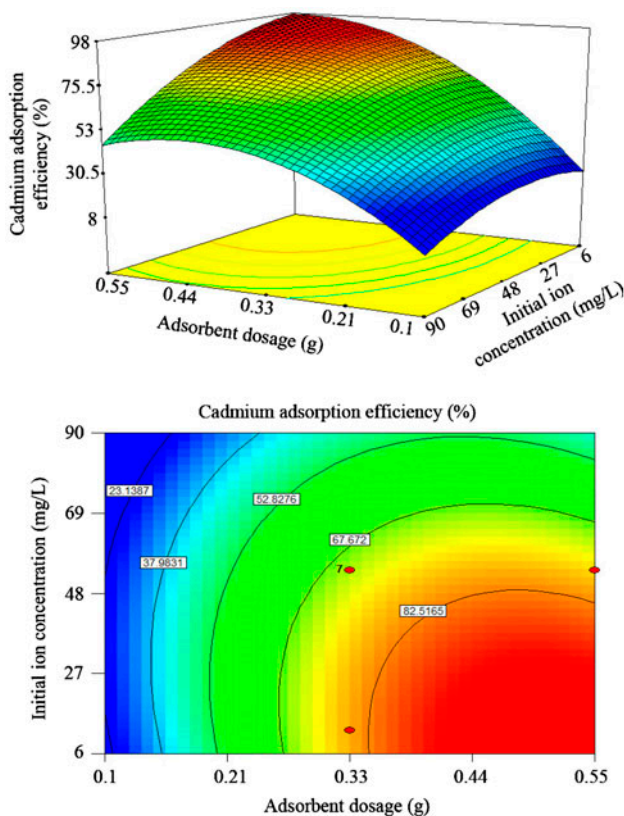


Fig. 4. Response surface and contour plots of interaction effects of adsorbent dosage and initial ion concentration on Cd(II) adsorption.

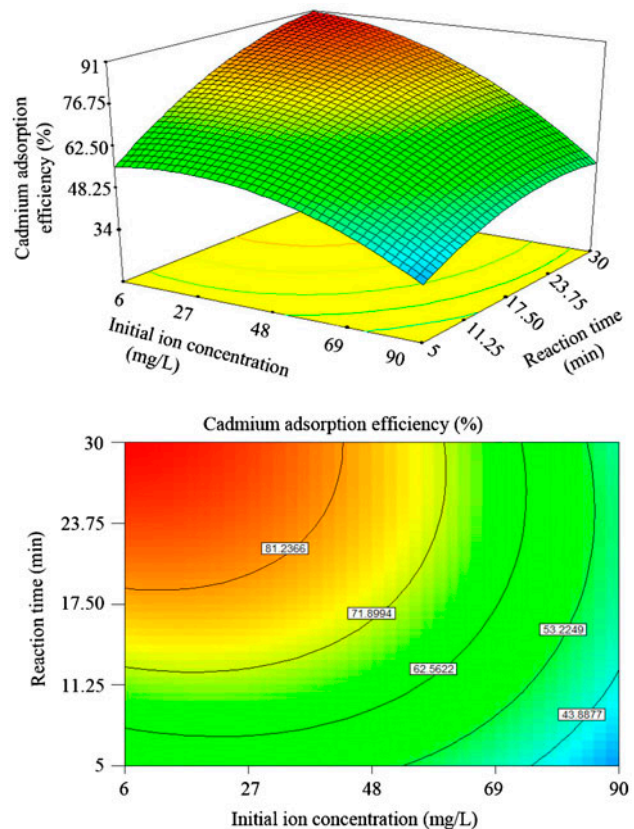


Fig. 5. Response surface and contour plots of interaction effects of reaction time and initial ion concentration on Cd(II) adsorption.

experimental conditions. Each surface and contour plot was drawn based on the combined effects of two variables against the adsorption efficiency of Cd(II). Fig. 3 shows contour and surface plots of the interaction effects of reaction time and adsorbent dosage on Cd(II) removal efficiency. From this figure, it can be observed that the maximum removal efficiency of Cd(II) was obtained in 30-min reaction time. This observation can be attributed to an increase in the availability of reactive sites to contaminants as a result of increasing the time period. At the first steps of the reaction, the interaction between the adsorbent and the adsorbate was quiet high, but it decreased in final time steps mainly due to the saturation of the adsorbents' surface area.

The interaction effects of the adsorbent dosage and the initial concentration of Cd(II) are illustrated in Fig. 4. Accordingly, a sharp enhancement was observed in the adsorption efficiency of Cd(II) upon increasing the concentration of adsorbent from 0.1 to 0.55 g. It is logical that in low adsorbent concentrations, fewer reactive sites are present to adsorb contaminants, while by increasing the amount of adsorbent, the rate of reactive sites will enhance, which leads to an enhancement in the efficiency of adsorbent [54]. Murugesan et al. [55] reported that the removal efficiency of Cd(II) increased significantly by increasing the concentration of polyazomethineamides as an adsorbent from 0.4 to 2 g/L [55].

In any batch system, the initial contaminant concentration always governs the removal efficiency. Fig. 5 illustrates the dependency of the adsorption of Cd(II) on the interaction influences of the reaction time and the initial ion concentration. Accordingly, the adsorption of Cd(II) has decreased significantly as a results of increasing the initial ion concentration. The decrease in the performance of adsorbent for the adsorption of Cd(II) through thickening the solution is generally attributed to the filling of the reactive site onto the surfaces of the adsorbent [56]. Anbia and Ghassemian [57] also stated that the removal efficiency of Cd(II) using mesoporous silicate was dropped by increasing the initial Cd(II) concentration in solution from 50 to 1,000 mg/L [57].

3.4. Process optimization and verification of the model's applicability

The principal aim of this study was to arrive at the optimal condition of Cd(II) adsorption using SDS-modified magnetite nanoparticles. The optimum values of the experimental parameters of Cd(II) removal were obtained at adsorbent dosage of 3.5 g, initial ion concentration of 30 mg/L, and reaction time of 30 min. In order to verify

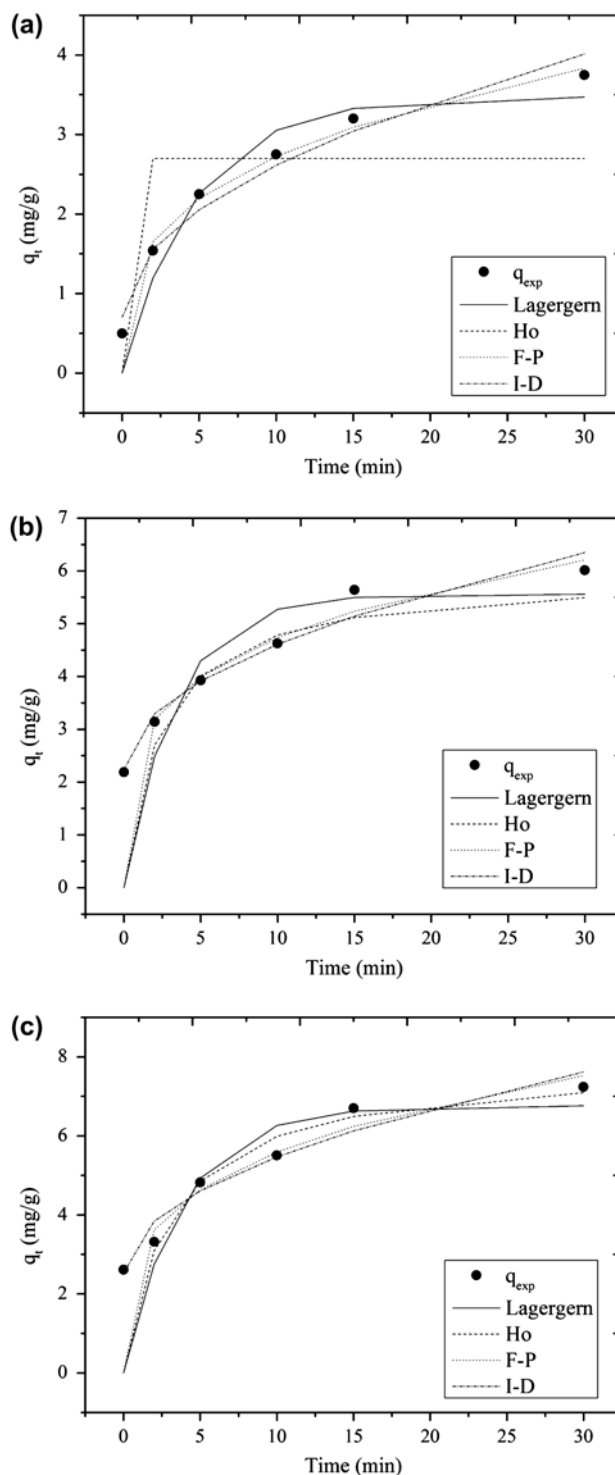


Fig. 6. Kinetic diagrams of Cd(II) adsorption onto SDS-MNP at different initial Cd(II) concentrations: (a) 10 mg/L, (b) 25 mg/L and (c) 50 mg/L.

the obtained predicted results, a similar experiment was performed with the same experimental variables. Results of the optimization studies show the validity of CCD

model through a big similarity between the predicted value (89.59%) of Cd(II) adsorption efficiency and the experimental value (91.07%). Ultimately, a good agreement between the experimental and predicted values obtained from the model approves that CCD is a suitable approach for the optimization of Cd(II) experimental conditions.

3.5. Adsorption kinetics

In order to perform the kinetic survey of Cd(II) adsorption, Lagergren, Ho, F–P, and I–D kinetic models were applied. The diagrams of the kinetic study of Cd(II) adsorption at different initial concentrations are

depicted in Fig. 6, which was simulated with 95% confidence bounds using nonlinear equations of Lagergren, Ho, F–P function, and Weber–Morris I–D kinetic models. Table 6 demonstrates the obtained parameter of kinetic models as well as their coefficients of determination at different initial Cd(II) concentrations. Based on Table 6, increasing the initial Cd(II) concentration from 10 to 50 mg/L leads to an abrupt enhancement in the quantity of q in Lagergren model from 2.94 to 5.03 mg/g. In Ho kinetic model, during a similar Cd(II) concentration, q increased likewise from 2.69 to 7.71 mg/g. Miretzky et al. [58] reported an enhancing trend in the adsorption capacity of pseudo-second-order kinetic model for the

Table 6
Adsorption kinetic parameters for Cd(II) adsorption onto SDS-MNP

Kinetic model	Parameters	Initial Cd(II) concentration (mg/L)		
		10	25	50
Lagergren	K_f (1/min)	0.20	0.29	0.26
	q_e (mg/g)	3.47	5.56	6.76
	R^2	0.899	0.30	0.40
	RMSE	0.37	1.22	1.41
Ho	k_s (mg/g min)	–2.621e+005	0.06	0.04
	q_e (mg/g)	2.69	6.33	7.81
	R^2	0.431	0.391	0.465
	RMSE	0.88	1.14	1.33
Fractional power	a (mg/g min ^b)	1.33	2.68	3.00
	b	0.31	0.24	0.26
	R^2	0.948	0.41	0.459
	RMSE	0.26	1.12	1.345
Intraparticle diffusion	C	0.70	2.23	2.53
	k_{id} (mg/g min ^{0.5})	0.60	0.75	0.92
	R^2	0.965	0.955	0.940
	RMSE	0.21	0.30	0.44

Table 7
The equilibrium contact time of Cd(II) adsorption by means of various adsorbents

Adsorbent	Equilibrium contact time (min)	Adsorption capacity (mg/g)	References
Pinuspinaster bark	120	7	[59]
Natural rice husk	60–120	73.96	[60]
Ground pine cone	500	15.345	[61]
<i>Azadirachta indica</i> (Neem) leaf powder	300	86.2	[62]
Acrylonitrile grafted-corn stalk	40	22.17	[63]
Sodium hydroxide modified-spent grain	120	17.3	[64]
Sodium dodecyl sulfate modified-magnetite nanoparticles	30	6.6	This study

removal of Cd(II) as the initial ion increased from 0.178 to 0.365 mM [58]. In a low Cd(II) concentration, all previously studied kinetic models showed high coefficients of determination, except for the Ho model. However, in high Cd(II) concentrations (i.e., 25 and 50 mg/L), only I-D model exhibited high coefficients of determination and low RMSE. Our findings showed that the I-D model was the most appropriate kinetic model to fit the experimental data of Cd(II) adsorption. Various equilibrium contact times of Cd(II) adsorption using different adsorbents are given in Table 7. Accordingly, with regard to other equilibrium contact times, the applied adsorbent in the present study could potentially be used as a feasible and efficient adsorbent to remove Cd(II) from aqueous solutions in a short time period.

3.6. Adsorption isotherm

The isotherm investigation of cadmium adsorption using modified magnetite nanoparticles was conducted at different adsorbent dosages (0.1, 0.2, and 0.25 g) employing Langmuir, Freundlich, L–F, and R–P nonlinear models. The models were evaluated via model coefficients of determination (R^2) and RMSE. The nonlinear plots of the applied isotherm models at various adsorbent dosages are illustrated in Fig. 7, based on the equilibrium Cd(II) concentration (C_e) against the adsorption capacity (q_e). The obtained parameters of isotherm models are reported in Table 8. As seen in this table, a sharp decrease is obvious in the quantity of Langmuir and L–F maxima q_{max} as the concentration of applied adsorbents increased. The obtained coefficients of determination in Langmuir model were in the range of 0.45–0.65, and the RMSE values were from 0.87 to 1.23, showing the lack of suitability of this model to fit the data of Cd(II) removal and data prediction. Other isotherm models (i.e., Freundlich, R–P, and L–F), on the other hand, give the best fit with extremely high coefficients of determination (>0.9) and negligible RMSE in all adsorbent dosages. Additionally, the highest values of the coefficient of determination of Freundlich (>0.98) indicate that such a model could fit well with the experimental data of Cd(II) adsorption. Previous studies have also reported that the Freundlich isotherm is the best model for the experimental data of Cd(II) adsorption [58,65]. Furthermore, from the findings of the isotherm study, it can be concluded that the capability of the employed models to fit the Cd(II) adsorption can be expressed as follows:

Freundlich > Redlich-Peterson > Langmuir–Freundlich > Langmuir

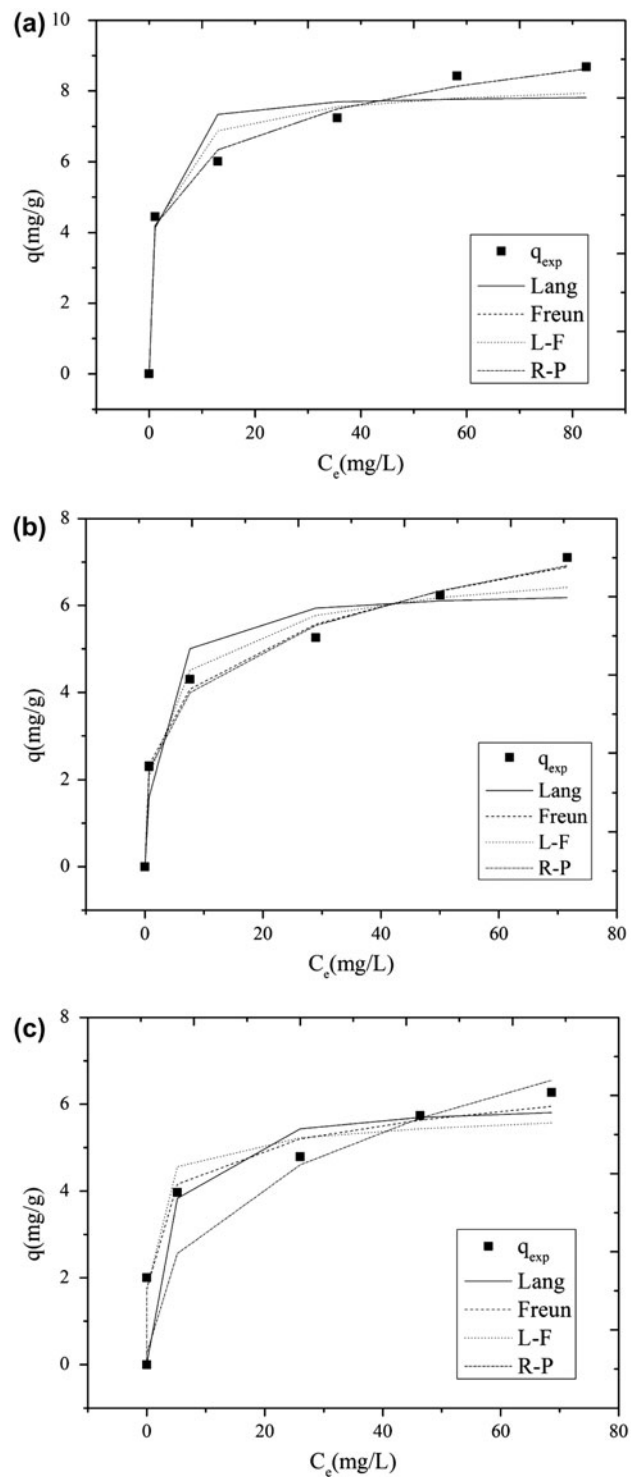


Fig. 7. Isotherm curves of Cd(II) adsorption onto SDS-magnetite nanoparticles at different SDS-MNP dosages: (a) 0.1 g, (b) 0.2 g and (c) 0.25 g.

The parameter “ n ” implies an abnormality from the linearity of the adsorption process. This parameter represents the extent of nonlinearity between the

Table 8
Adsorption isotherm constants and coefficients of determination for Cd(II) adsorption onto SDS-MNP

Isotherm model	Parameters	Adsorbent dosage (g)		
		0.1	0.2	0.25
Freundlich	k_f (mg/g) (mg/L) ⁻ⁿ	4.13	2.52	3.31
	n	6.00	4.26	7.21
	R^2	0.994	0.985	0.966
	RMSE	0.28	0.26	0.35
Langmuir	q_{\max} (mg/g)	7.90	6.36	6.06
	b (L/mg)	0.99	0.48	0.33
	R^2	0.938	0.833	0.594
	RMSE	1.04	0.87	1.23
Langmuir–Freundlich	q_{\max} (mg/g)	8.65	7.73	7.10
	b (L/mg)	0.81	0.23	1.63
	n	0.57	0.55	0.27
	R^2	0.956	0.920	0.859
	RMSE	0.67	0.52	0.62
Redlich–Peterson	K_R	16,240	14,820	14,510
	a_R	3,927	6,107	10,310
	β	0.83	0.75	0.63
	R^2	0.994	0.983	0.54
	RMSE	0.32	0.33	0.43

concentration of the adsorbate and the adsorbent as follows: if $n < 1$, the adsorption process is potentially physisorption; if $n = 1$, the adsorption is therefore linear; and if $n > 1$, then the adsorption process is definitely chemisorption. Having a closer look at Table 8, we see that parameter “ n ” is higher than 1, which shows that Cd(II) adsorption onto the surfaces of magnetite nanoparticles was in a favorable experimental condition and was intrinsically a chemisorption process.

4. Conclusions

In this study, the adsorption of Cd(II) in aqueous solutions using SDS-modified magnetite nanoparticles was optimized using CCD as one the most well-known designs of RSM under different input variables including the reaction time, the adsorbent dosage, and the initial ion concentration. The optimization results revealed that initial ion concentration, adsorbent dosage, and the quadratic effect of initial ion concentration had great impacts on Cd(II) removal. The optimum condition for the removal of Cd(II) was obtained at the reaction time of 30 min with 0.35 g of the adsorbent and 30 mg/L of the initial ion concentration. Furthermore, the data of Cd(II) adsorption were interpreted using different kinetic and isotherm models. After employing kinetic

investigations on Cd(II) adsorption, it was found that the I-D, compared to other kinetic models, was more efficient to fit the experimental data. The findings of the isotherm studies showed that among all the applied isotherm models, the data of Cd(II) removal could better be described by Freundlich than by Langmuir, R–P, and L–F. Finally, it can be concluded that SDS-MNP might serve as an efficient adsorbent mainly due to a high surface area as well as a high adsorption capacity for adsorptive removal of Cd(II) from contaminated aqueous solutions.

Acknowledgments

The financial support of the Environmental Technologies Research Center (ETRC) and the Research and Technology Deputy of Ahvaz Jundishapur University of Medical Sciences [grant number: ETRC9008] for the study are thankfully acknowledged.

References

- [1] K. Rout, M. Mohapatra, S. Anand, 2-Line ferrihydrite: Synthesis, characterization and its adsorption behaviour for removal of Pb(ii), Cd(ii), Cu(ii) and Zn(ii) from aqueous solutions, Dalton Trans. 41 (2012) 3302–3312.

- [2] P. Teymouri, A. Babaei, K. Ahmadi, N. Jaafarzadeh, Biosorption studies on NaCl-modified ceratophyllum demersum: Removal of toxic chromium from aqueous solution, *Chem. Eng. Commun.* 200 (2013) 1394–1413.
- [3] A. Babaei, Z. Baboli, N. Jaafarzadeh, G. Goudarzi, M. Bahrami, Synthesis, performance, and nonlinear modeling of modified nano-sized magnetite for removal of Cr(VI) from aqueous solutions, *Desalin. Water Treat.* (2013), 1–10, doi: 10.1080/19443994.2013.846238.
- [4] M. Bahrami, S. Boroomandnasab, H.A. Kashkuli, A. Farrokhian, A. Babaei, Removal of Cd(II) from aqueous solution using modified Fe₃O₄ nanoparticles, *Rep. Opin.* 4 (2012) 31–40.
- [5] D. Ghosh, R. Saha, A. Ghosh, R. Nandi, B. Saha, A review on toxic cadmium biosorption from contaminated wastewater, *Desalin. Water Treat.* (2013) 1–8, doi: 10.1080/19443994.2013.846233.
- [6] N. Jaafarzadeh, P. Teymouri, A. Babaei, N. Alavi, M. Ahmadi, Biosorption of Cadmium (II) from aqueous solution by NaCl-treated *Ceratophyllum demersum*, *Environ. Eng. Manage. J.* 13 (2014) 763–773.
- [7] Y.C. Sharma, Thermodynamics of removal of cadmium by adsorption on an indigenous clay, *Chem. Eng. J.* 145 (2008) 64–68.
- [8] A.B. Pérez-Marín, V.M. Zapata, J.F. Ortuño, M. Aguilar, J. Sáez, M. Lloréns, Removal of cadmium from aqueous solutions by adsorption onto orange waste, *J. Hazard. Mater.* 139 (2007) 122–131.
- [9] Z. Elouear, J. Bouzid, N. Boujelben, M. Feki, F. Jamoussi, A. Montiel, Heavy metal removal from aqueous solutions by activated phosphate rock, *J. Hazard. Mater.* 156 (2008) 412–420.
- [10] V.K. Gupta, I. Ali, T.A. Saleh, A. Nayak, S. Agarwal, Chemical treatment technologies for waste-water recycling—An overview, *RSC. Adv.* 2 (2012) 6380–6388.
- [11] V.K. Gupta, I. Ali, V.K. Saini, Defluoridation of wastewaters using waste carbon slurry, *Water Res.* 41 (2007) 3307–3316.
- [12] V.K. Gupta, S. Agarwal, T.A. Saleh, Synthesis and characterization of alumina-coated carbon nanotubes and their application for lead removal, *J. Hazard. Mater.* 185 (2011) 17–23.
- [13] A. Mittal, L. Kurup (Krishnan), V.K. Gupta, Use of waste materials—Bottom ash and de-oiled soya, as potential adsorbents for the removal of Amaranth from aqueous solutions, *J. Hazard. Mater.* 117 (2005) 171–178.
- [14] V.K. Gupta, A. Mittal, L. Kurup, J. Mittal, Adsorption of a hazardous dye, erythrosine, over hen feathers, *J. Colloid Interface Sci.* 304 (2006) 52–57.
- [15] V.K. Gupta, A. Mittal, L. Krishnan, J. Mittal, Adsorption treatment and recovery of the hazardous dye, brilliant blue FCF, over bottom ash and de-oiled soya, *J. Colloid Interface Sci.* 293 (2006) 16–26.
- [16] V.K. Gupta, R. Jain, S. Varshney, Removal of reactofix golden yellow 3 RFN from aqueous solution using wheat husk—An agricultural waste, *J. Hazard. Mater.* 142 (2007) 443–448.
- [17] V.K. Gupta, A. Mittal, A. Malviya, J. Mittal, Adsorption of carmoisine A from wastewater using waste materials—Bottom ash and deoiled soya, *J. Colloid Interface Sci.* 335 (2009) 24–33.
- [18] A. Mittal, J. Mittal, A. Malviya, D. Kaur, V.K. Gupta, Adsorption of hazardous dye crystal violet from wastewater by waste materials, *J. Colloid Interface Sci.* 343 (2010) 463–473.
- [19] V.K. Gupta, A. Rastogi, A. Nayak, Biosorption of nickel onto treated alga (*Oedogonium hatei*): Application of isotherm and kinetic models, *J. Colloid Interface Sci.* 342 (2010) 533–539.
- [20] A. Mittal, V.K. Gupta, A. Malviya, J. Mittal, Process development for the batch and bulk removal and recovery of a hazardous, water-soluble azo dye (Metanil Yellow) by adsorption over waste materials (bottom ash and de-oiled soya), *J. Hazard. Mater.* 151 (2008) 821–832.
- [21] V.K. Gupta, B. Gupta, A. Rastogi, S. Agarwal, A. Nayak, A comparative investigation on adsorption performances of mesoporous activated carbon prepared from waste rubber tire and activated carbon for a hazardous azo dye—Acid Blue 113, *J. Hazard. Mater.* 186 (2011) 891–901.
- [22] A.K. Jain, V.K. Gupta, A. Bhatnagar, Suhas, A comparative study of adsorbents prepared from industrial wastes for removal of dyes, *Sep. Sci. Technol.* 38 (2003) 463–481.
- [23] V.K. Gupta, S. Sharma, Removal of zinc from aqueous solutions using bagasse fly ash—A low cost adsorbent, *Ind. Eng. Chem. Res.* 42 (2003) 6619–6624.
- [24] T.A. Saleh, V.K. Gupta, Column with CNT/magnesium oxide composite for lead(II) removal from water, *Environ. Sci. Pollut. Res.* 19 (2012) 1224–1228.
- [25] G.Q. Tan, D. Xiao, Adsorption of cadmium ion from aqueous solution by ground wheat stems, *J. Hazard. Mater.* 164 (2009) 1359–1363.
- [26] B. Benguella, H. Benaissa, Cadmium removal from aqueous solutions by chitin: Kinetic and equilibrium studies, *Water Res.* 36 (2002) 2463–2474.
- [27] G. Crini, Recent developments in polysaccharide-based materials used as adsorbents in wastewater treatment, *Prog. Polym. Sci.* 30 (2005) 38–70.
- [28] Y.T. Meng, Y.M. Zheng, L.M. Zhang, J.Z. He, Biogenic Mn oxides for effective adsorption of Cd from aquatic environment, *Environ. Pollut.* 157 (2009) 2577–2583.
- [29] R.D.C. Soltani, A.J. Jafari, G.H.S. Khorramabadi, Investigation of cadmium (II) ions biosorption onto pretreated dried activated sludge, *Am. J. Environ. Sci.* 5 (2009) 41–46.
- [30] L. Semerjian, Equilibrium and kinetics of cadmium adsorption from aqueous solutions using untreated *Pinus halepensis* sawdust, *J. Hazard. Mater.* 173 (2010) 236–242.
- [31] Z. Li, T. Katsumi, S. Imaizumi, X. Tang, T. Inui, Cd(II) adsorption on various adsorbents obtained from charred biomaterials, *J. Hazard. Mater.* 183 (2010) 410–420.
- [32] V.K. Gupta, C.K. Jain, I. Ali, M. Sharma, V.K. Saini, Removal of cadmium and nickel from wastewater using bagasse fly ash—A sugar industry waste, *J. Hazard. Mater.* 37 (2003) 4038–4044.
- [33] H.R. Tashauoei, H.M. Attar, M.M. Amin, M. Kamali, M. Nikaeen, M.V. Dastjerdi, Removal of cadmium and humic acid from aqueous solutions using surface modified nanozeolite, *Int. J. Environ. Sci. Technol.* 7 (2010) 497–508.
- [34] M. Visa, C. Bogatu, A. Duta, Simultaneous adsorption of dyes and heavy metals from multicomponent solutions using fly ash, *Appl. Surf. Sci.* 256 (2010) 5486–5491.

- [35] D.W. Elliott, W.X. Zhang, Field assessment of nano-scale biometallic particles for groundwater treatment, *Environ. Sci. Technol.* 35 (2001) 4922–4926.
- [36] A.R. Esfahani, S. Hojati, A. Azimi, L. Alidokht, A.R. Khataee, M. Farzadian, Reductive removal of hexavalent chromium from aqueous solution using sepiolite-stabilized zero-valent iron nanoparticles: Process optimization and kinetic studies, *Korean J. Chem. Eng.* 31 (2014) 630–638.
- [37] G. Kataby, M. Cojocaru, R. Prozorov, A. Gedanken, Coating carboxylic acids on amorphous iron nanoparticles, *Langmuir* 15 (1999) 1703–1708.
- [38] A.R. Esfahani, A.F. Firouzi, G. Sayyad, A. Kiasat, L. Alidokht, A.R. Khataee, Pb(II) removal from aqueous solution by polyacrylic acid stabilized zero-valent iron nanoparticles: Process optimization using response surface methodology, *Res. Chem. Intermed.* 40 (2014) 431–445.
- [39] A.R. Esfahani, A.F. Firouzi, G. Sayyad, A.R. Kiasat, Transport and retention of polymer-stabilized zero-valent iron nanoparticles in saturated porous media: Effects of initial particle concentration and ionic strength, *J. Ind. Eng. Chem.* 20 (2014) 2671–2679.
- [40] A.A. Babaei, A.R. Mesdaghinia, N.J. Haghghi, R. Nabizadeh, A.H. Mahvi, Modeling of nonylphenol degradation by photo-nanocatalytic process via multivariate approach, *J. Hazard. Mater.* 185 (2011) 1273–1279.
- [41] A. Ditsch, P.E. Laibinis, D.I.C. Wang, T.A. Hatton, Controlled clustering and enhanced stability of polymer-coated magnetic nanoparticles, *Langmuir* 21 (2005) 6006–6018.
- [42] M. Taheri, M.R. AlaviMoghaddam, M. Arami, Optimization of acid black 172 decolorization by electrocoagulation using response surface methodology, *Iran. J. Environ. Health Sci. Engineer.* 9 (2012) 1–8.
- [43] S. Si, A. Kotal, T.K. Mandal, Size-controlled synthesis of magnetite nanoparticles in the presence of polyelectrolytes, *J. Chem. Mater.* 16 (2004) 3489–3496.
- [44] A. Günay, E. Arslankaya, İsmail Tosun, Lead removal from aqueous solution by natural and pretreated clinoptilolite: Adsorption equilibrium and kinetics, *J. Hazard. Mater.* 146 (2007) 362–371.
- [45] M.S. Chiou, H.Y. Li, Adsorption behavior of reactive dye in aqueous solution on chemical cross-linked chitosan beads, *Chemosphere* 50 (2003) 1095–1105.
- [46] R.C. Dalal, Desorption of soil phosphate by anion-exchange resin, *Commun. Soil Sci. Plant Anal.* 5 (1974) 531–538.
- [47] W.J. Weber, J.C. Morris, Kinetics of adsorption on carbon from solution, *J. Sanit. Eng. Div. Am. Soc. Civ. Eng.* 89 (1963) 31–60.
- [48] A.K. Abdessalem, N. Oturan, N. Bellakhal, M. Dachraoui, M.A. Oturan, Experimental design methodology applied to electro-Fenton treatment for degradation of herbicide chlortoluron, *Appl. Catal., B* 78 (2008) 334–341.
- [49] H. Hasar, Adsorption of nickel(II) from aqueous solution onto activated carbon prepared from almond husk, *J. Hazard. Mater.* 97 (2003) 49–57.
- [50] E. Turiel, C. Perez-Conde, A. Martin-Esteban, Assessment of the cross reactivity and binding sites characterization of a propazine-imprinted polymer using the Langmuir–Freundlich isotherm, *The Analyst* 128 (1993) 137–141.
- [51] Y.S. Ho, C.C. Chiang, Sorption studies of acid dye by mixed sorbents, *Adsorption* 7 (2001) 139–147.
- [52] M.A. Bezerra, R.E. Santelli, E.P. Oliveira, L.S. Villar, L.A. Escalera, Response surface methodology (RSM) as a tool for optimization in analytical chemistry, *Talanta* 76 (2008) 965–977.
- [53] J.R. Memon, S.Q. Memon, M.I. Bhangar, M.Y. Khuhawar, G.C. Allen, G.Z. Memon, A.G. Pathan, Efficiency of Cd(II) removal from aqueous media using chemically modified polystyrene foam, *Eur. Polym. J.* 44 (2008) 1501–1511.
- [54] Q. Tang, X. Tang, M. Hu, Z. Li, Y. Chen, P. Lou, Removal of Cd(II) from aqueous solution with activated *Firmiana Simplex* leaf: Behaviors and affecting factors, *J. Hazard. Mater.* 179 (2010) 95–103.
- [55] A. Murugesan, L. Ravikumar, V. SathyaSelvaBala, P. Senthikumar, T. Vidhyadevi, S. Dinesh Kirupha, S.S. Kalaivani, S. Krithiga, S. Sibanesan, Removal of Pb(II), Cu(II) and Cd(II) ions from aqueous solution using polyazomethineamides. Equilibrium and kinetic approach, *Desalination* 271 (2011) 199–208.
- [56] D.C. Perekh, J.B. Patel, P. Sudhakar, V.J. Koshy, Removal of trace metals with mango seed powder, *Indian J. Chem. Technol.* 9 (2002) 540–542.
- [57] M. Anbia, Z. Ghassemian, Removal of Cd(II) and Cu(II) from aqueous solutions using mesoporous silicate containing zirconium and iron, *Chem. Eng. Res. Des.* 89 (2011) 2770–2775.
- [58] P. Miretzky, C. Muñoz, A. Carrillo-Chavez, Cd (II) removal from aqueous solution by *Eleocharis acicularis* biomass, equilibrium and kinetic studies, *Bioresour. Technol.* 101 (2010) 2637–2642.
- [59] G. Vázquez, J.A. González-Álvarez, S. Freire, M. López-Lorenzo, G. Antorrena, Removal of cadmium and mercury ions from aqueous solution by sorption on treated *Pinus pinaster* bark: Kinetics and isotherms, *Bioresour. Technol.* 82 (2002) 247–251.
- [60] H. Ye, Q. Zhu, D. Du, Adsorptive removal of Cd(II) from aqueous solution using natural and modified rice husk, *Bioresour. Technol.* 101 (2010) 5175–5179.
- [61] H. Izanloo, S. Nasser, Cadmium removal from aqueous solutions by ground pine cone, *Iran. J. Environ. Health Sci. Eng.* 2 (2005) 33–42.
- [62] A. Sharma, K.G. Bhattacharyya, *Azadirachta indica* (Neem) leaf powder as a biosorbent for removal of Cd (II) from aqueous medium, *J. Hazard. Mater.* 125 (2005) 102–112.
- [63] L. Zheng, Z. Dang, C. Zhu, X. Yi, H. Zhang, C. Liu, Removal of cadmium(II) from aqueous solution by corn stalk graft copolymers, *Bioresour. Technol.* 101 (2010) 5820–5826.
- [64] K.S. Low, C.K. Lee, S.C. Liew, Sorption of cadmium and lead from aqueous solutions by spent grain, *Process Biochem.* 36 (2000) 59–64.
- [65] D. Ozdes, C. Duran, H.B. Senturk, Adsorptive removal of Cd(II) and Pb(II) ions from aqueous solutions by using Turkish illitic clay, *J. Environ. Manage.* 92 (2011) 3082–3090.